
Tumor Uptake of ^{64}Cu -DOTA-Trastuzumab in Patients with Metastatic Breast Cancer

Joanne E. Mortimer¹, James R. Bading¹, Jinha M. Park², Paul H. Frankel³, Mary I. Carroll¹, Tri T. Tran², Erasmus K. Poku⁴, Russell C. Rockne³, Andrew A. Raubitschek⁴, John E. Shively⁵, and David M. Colcher⁴

¹Department of Medical Oncology and Experimental Therapeutics, City of Hope, Duarte, California; ²Department of Radiology, City of Hope, Duarte, California; ³Department of Information Sciences, City of Hope, Duarte, California; ⁴Department of Cancer Immunotherapy and Tumor Immunology, Beckman Research Institute of the City of Hope, Duarte, California; and ⁵Department of Immunology, Beckman Research Institute of the City of Hope, Duarte, California

The goal of this study was to characterize the relationship between tumor uptake of ^{64}Cu -DOTA-trastuzumab as measured by PET/CT and standard, immunohistochemistry (IHC)-based, histopathologic classification of human epidermal growth factor receptor 2 (HER2) status in women with metastatic breast cancer (MBC). **Methods:** Women with biopsy-confirmed MBC and not given trastuzumab for 2 mo or more underwent complete staging, including ^{18}F -FDG PET/CT. Patients were classified as HER2-positive (HER2+) or -negative (HER2-) based on fluorescence in situ hybridization (FISH)-supplemented immunohistochemistry of biopsied tumor tissue. Eighteen patients underwent ^{64}Cu -DOTA-trastuzumab injection, preceded in 16 cases by trastuzumab infusion (45 mg). PET/CT was performed 21–25 (day 1) and 47–49 (day 2) h after ^{64}Cu -DOTA-trastuzumab injection. Radiolabel uptake in prominent lesions was measured as SUV_{max} . Average intrapatient SUV_{max} ($\langle \text{SUV}_{\text{max}} \rangle_{\text{pt}}$) was compared between HER2+ and HER2- patients. **Results:** Eleven women were HER2+ (8 immunohistochemistry 3+; 3 immunohistochemistry 2+/FISH amplified), whereas 7 were HER2- (3 immunohistochemistry 2+/FISH nonamplified; 4 immunohistochemistry 1+). Median $\langle \text{SUV}_{\text{max}} \rangle_{\text{pt}}$ for day 1 and day 2 was 6.6 and 6.8 g/mL for HER2+ and 3.7 and 4.3 g/mL for HER2- patients ($P < 0.005$ either day). The distributions of $\langle \text{SUV}_{\text{max}} \rangle_{\text{pt}}$ overlapped between the 2 groups, and interpatient variability was greater for HER2+ than HER2- disease ($P < 0.005$ and 0.001, respectively, on days 1 and 2). **Conclusion:** By 1 d after injection, uptake of ^{64}Cu -DOTA-trastuzumab in MBC is strongly associated with patient HER2 status and is indicative of binding to HER2. The variability within and among HER2+ patients, as well as the overlap between the HER2+ and HER2- groups, suggests a role for ^{64}Cu -DOTA-trastuzumab PET/CT in optimizing treatments that include trastuzumab.

Key Words: antibody; breast cancer; PET; HER2; clinical trial

J Nucl Med 2018; 59:38–43

DOI: 10.2967/jnumed.117.193888

Human epidermal growth factor receptor 2 (HER2) is an important target in the treatment of breast cancer. Eligibility for

HER2-directed therapy is determined from a biopsy of primary or metastatic tumor. Patients whose tumors demonstrate 3+ staining by immunohistochemistry (IHC) or gene amplification by fluorescence in situ hybridization (FISH) are considered HER2-positive (HER2+) and are candidates for HER2-directed therapies such as trastuzumab and ado-trastuzumab emtansine (T-DM1) (1). The addition of anti-HER2 treatment to chemotherapy improves patient survival for all stages of HER2+ breast cancer (2).

Because HER2-directed therapies are costly and potentially toxic, it is important to determine which patients are likely to benefit from these treatments. The current selection method is only modestly successful in predicting response or outcome for patients receiving HER2-directed therapy. This is especially true in metastatic breast cancer (MBC), where response rates for first- and second-line treatments are typically 50%–80% and 25%–50%, respectively, and most initial responders experience disease progression within 2 y after starting treatment (3). Furthermore, some HER2-negative (HER2-) patients benefit from anti-HER2 therapy (4).

Several factors limit the predictive accuracy of pathologic HER2 assessment. These assessments are usually based on core-needle biopsy of a single lesion and thus may suffer from sampling error due to heterogeneous intratumoral distribution of HER2, as well as variable HER2 expression among multiple tumors in the same patient. Furthermore, high HER2 expression or gene amplification does not guarantee efficacy for anti-HER2 therapy. The cancer may have molecular mechanisms of resistance to the therapeutic agents (5). More fundamentally, response requires that the therapeutic agents be delivered to and incorporated by tumor cells in sufficient quantities. Solid tumors often develop in ways that hinder delivery of blood-borne molecules to tumor cells (6). This is especially true for macromolecules such as antibodies, which distribute from blood into tissue by convection rather than diffusion.

We are developing PET imaging with ^{64}Cu -DOTA-trastuzumab for the purpose of measuring tumor uptake of trastuzumab in patients with breast cancer. We have shown that ^{64}Cu -DOTA-trastuzumab PET/CT is highly effective in visualizing tumors in women with HER2+ MBC ($n = 8$) and that trastuzumab (45 mg) administered before ^{64}Cu -DOTA-trastuzumab decreases hepatic uptake of ^{64}Cu about 75%, without affecting tumor uptake (7). We report here on our efforts to characterize the relationship between tumor uptake of ^{64}Cu -DOTA-trastuzumab and standard classification of HER2 status for MBC. For that, we enrolled women with HER2- disease, as well as additional women with HER2+ MBC.

Received Mar. 24, 2017; revision accepted May 31, 2017.

For correspondence or reprints contact: Joanne Mortimer, Department of Medical Oncology & Experimental Therapeutics, City of Hope Comprehensive Cancer Center, 1500 East Duarte Rd., Duarte, CA 91010.

E-mail: jmortimer@coh.org

Published online Jun. 21, 2017.

COPYRIGHT © 2018 by the Society of Nuclear Medicine and Molecular Imaging.

MATERIALS AND METHODS

Patient Selection

Women with MBC outside the breast and regional lymphatics and no exposure to trastuzumab for at least 2 mo were considered for study participation after staging that included ^{18}F -FDG PET/CT. All candidates underwent biopsy of a metastatic lesion within 28 d before the ^{64}Cu -DOTA-trastuzumab procedure to confirm recurrent disease and assess HER2 status. Immunohistochemical staining was performed on all specimens, and those scored IHC 2+ also underwent FISH. To support accurate PET-derived measurement of ^{64}Cu -DOTA-trastuzumab uptake in tumors, disease outside the breast/axillary region and biopsy site that measured 2.0 cm or more was also required. Accrual extended from March 2011 through September 2013. The study was approved by the City of Hope Institutional Review Board, and all patients provided written informed consent before study participation.

^{64}Cu -DOTA-Trastuzumab Preparation and Administration

^{64}Cu (half-life, 12.8 h; 0.18 positrons/decay) was provided by the Mallinckrodt Institute of Radiology, Washington University School of Medicine. Radiolabeled trastuzumab was prepared according to an investigational new drug application (IND 109971). The procedure includes heating at 43°C for 45 min followed by incubation with an excess of diethylenetriaminepentaacetic acid, which eliminates ^{64}Cu binding to secondary chelating sites on the antibody while maintaining the immunoreactivity of the radiolabeled product (7). The ^{64}Cu -DOTA-trastuzumab (trastuzumab dose, 5 mg) was mixed with saline (25 mL) and administered intravenously over 10 min. Injected radioactivity was 364–551 MBq (mean, 464 MBq). Two patients in the initial study received no additional trastuzumab; the other 16 were given trastuzumab (45 mg) intravenously over 15 min immediately before administration of ^{64}Cu -DOTA-trastuzumab.

PET/CT Imaging

All images were acquired with the same Discovery STe 16 PET/CT scanner (GE Healthcare) operated in 3-dimensional mode (septal retracted). The PET axial field of view was 15.4 cm, with an image slice thickness of 3.3 mm. Consecutive bed positions overlapped by 11 slices. The PET images were reconstructed by the iterative, ordered-subsets expectation maximization method with gaussian postsmoothing and standard corrections for scanner dead time, random and scattered coincidence events, nonuniform detector sensitivity, and photon attenuation. Spatial resolution of the PET images as measured for an ^{18}F line source-in-water phantom was 9 mm in full width at half maximum.

Patients underwent standard ^{18}F -FDG PET/CT 1–17 d before the ^{64}Cu -DOTA-trastuzumab procedure. They fasted for 6 h or more before injection of ^{18}F -FDG. In all cases, serum glucose concentration met institutional requirements (≤ 120 mg/dL for nondiabetic patients, ≤ 200 mg/dL for diabetic patients). Injected activity and time from injection to scan ranged from 407 to 596 MBq (mean, 518 MBq) and 50–72 min, respectively.

Axial coverage in the ^{64}Cu PET scans was based on tumor location as determined from the preceding ^{18}F -FDG PET/CT examination. Scan duration for ^{64}Cu was 60 min, except 1 scan that was terminated at 40 min because of patient discomfort. To allow accumulation of the radiolabeled antibody in tumor, the first (day 1) scan was obtained 21–25 h after injection. For all but 1 patient, a second (day 2) scan was obtained 47–49 h after injection. Day-1 scans comprised 3 or 4 bed positions (20 or 15 min each) and day-2 scans 1 or 2 bed positions (60 or 30 min each), depending on patient body thickness. Multiple bed positions were acquired contiguously, except for 2 patients for whom the scans were made partially discontinuous to increase disease coverage.

Image Analysis

Scans were interpreted by an expert radiologist. Tumors and other anatomic features were considered PET-positive if visualized with

positive contrast relative to adjacent tissue. Lesionlike, PET-positive findings were disregarded if CT was judged inconclusive.

Image analysis was performed with XD (version 3.6; Mirada Medical). Radiolabel uptake for tumors was measured in terms of single-voxel maximum SUV (SUV_{max} ; $\text{SUV} = \text{tissue activity per mL} \times \text{body weight [g]} / \text{injected activity decay-corrected to time of scan}$). A detailed description of the criteria used in judging the suitability of tumor images for measurement of SUV_{max} , as well as the methods used to define the volumes of interest within which SUV_{max} was determined, is provided in the supplemental materials (available at <http://jnm.snmjournals.org>). In brief, SUV_{max} was measured for lesions that were identifiable on CT and for which the PET maximum voxel was clearly associated with the CT correlate, and not overlapped by the image of an adjacent PET-positive feature (e.g., vessel, organ, tumor). The number of lesions evaluated per patient was limited to 10. Measurements excluded the 2 transaxial slices at either end of a scan, where random noise tends to be excessive because of low detection sensitivity. Biopsied tumors were excluded a priori from the analysis because of possible effect of the biopsy procedure on radiotracer uptake. The data suggest higher uptake in biopsied tumors. Conclusions were not altered when the biopsy sites were included in the analysis (data not shown).

Measurements of ^{64}Cu activity in blood were obtained from PET images of the cardiac ventricles. Mean SUVs were determined for regions of interest of fixed size placed well within the ventricle boundaries on 3 contiguous transaxial image slices.

Tumor size was estimated from ^{18}F -FDG images. Volumes of interest were defined for those images using a maximum voxel-based thresholding technique (8), with the 3-dimensional isocontour tailored to approximate the boundary of the tumor CT image. Details of the analysis are given in the supplemental materials.

Statistical Analysis

The study was designed to accrue at least 8 HER2+ and 7 HER2– patients. This plan provided 80% power to detect an effect = 1.36 \times the common SD of SUV_{max} with a 1-sided significance level of 0.05 when comparing ^{64}Cu -DOTA-trastuzumab uptake between the HER2+ and HER2– groups. The actual accrual of HER2+ patients was 11 during the course of enrolling 7 HER2– patients, resulting in greater-than-planned power.

We used mean inpatient SUV_{max} ($\langle \text{SUV}_{\text{max}} \rangle_{\text{pt}}$) as the primary metric for patient-level comparisons. We also compared uptake between the HER2+ and HER2– groups, treating SUV_{max} measurements for individual tumors as independent observations. Because they are skewed, we characterized $\langle \text{SUV}_{\text{max}} \rangle_{\text{pt}}$ and SUV_{max} distributions in terms of median rather than mean values. Statistical significance of differences in $\langle \text{SUV}_{\text{max}} \rangle_{\text{pt}}$ and SUV_{max} between patient groups was assessed via a nonparametric (Wilcoxon rank-sum) test.

We also compared inter- and inpatient variability of tumor uptake of ^{64}Cu -DOTA-trastuzumab between the HER2+ and HER2– groups. The coefficient of variation for $\langle \text{SUV}_{\text{max}} \rangle_{\text{pt}}$ was compared using both an F test and a Wilcoxon rank-sum test. The Wilcoxon test was used to compare inpatient coefficients of variation of SUV_{max} between the 2 patient groups. Linear models were used to consider the effect of lesion site.

All significance testing was 2-sided, with a *P* value of less than 0.05 considered statistically significant.

RESULTS

Patients

Participating patients are described in Table 1. The HER2+ group (*n* = 11) includes the 8 women from our initial feasibility study (7). The HER2+ and HER2– groups were closely similar with regard to age and hormone receptor status. Of the 8 women

TABLE 1
Patient Demographics and Clinical Characteristics

Characteristic	HER2+ (n = 11)	HER2- (n = 7)
Median age (y)	59 y (age range, 35–75 y)	61 y (age range, 40–71 y)
Hormone receptor and HER2 status of recurrent disease		
ER and PR receptors		
ER- and/or PR-positive	6	
ER- and PR-negative	5	
HER2		
IHC1+		
IHC2+	3	
IHC3+	8	
Prior HER2-directed therapy		
None	3	
Trastuzumab for metastasis	8 (79 d–36 mo)	
Sites of metastatic disease measured for SUV _{max}		
Bone	24	
Lymph nodes	23	
Liver	6	
Lung	6	
Other*	2	
Breast/chest wall†	5	
Tumor volume (cm ³)‡		
Mean	5.8	
SE	0.9	

*Pulmonary effusion (HER2+) or body wall outside breast region.

†Breast or chest wall adjacent to breast.

‡Volume within isocontour of ¹⁸F-FDG tumor image approximately matching boundary of CT correlate.

HER2 = human epidermal growth factor receptor 2; ER = estrogen receptor; PR = progesterone receptor; IHC = immunohistochemistry.

with HER2+ disease previously treated with trastuzumab, time between the last dose of the antibody and ⁶⁴Cu-DOTA-trastuzumab injection was 11 wk for one and at least 4 mo for all the others. Anatomic distribution of tumors for which uptake was measured was proportionately similar for HER2+ versus HER2- patients, with the biggest difference being 6 versus 0 liver metastases. Tumors were, on average, larger for HER2- than HER2+ patients. However, SUV_{max} for ⁶⁴Cu-DOTA-trastuzumab was not significantly related to tumor size for either group (Supplemental Fig. 1).

Tumor Uptake of ⁶⁴Cu-DOTA-Trastuzumab

Tumor uptake data are plotted in Figure 1. The number of lesions evaluated for days 1 and 2 were 58 and 46 for HER2+ patients versus 29 and 18 for HER2- patients. For a given patient,

the axial range of the scan was shortened between day 1 and 2, in general reducing the number of lesions evaluated on day 2. Some lesions were evaluable only on day 2 because of technical error or insufficient lesion-to-background contrast on day 1. One patient in the IHC1+ subgroup was not able to undergo scanning on day 2 and 1 patient in the IHC2+/FISH group had no lesions that were evaluable for SUV_{max} on day 1.

Tumor uptake of ⁶⁴Cu-DOTA-trastuzumab was, on average, higher in HER2+ than in HER2- patients, regardless of whether the data for individual lesions were grouped by patient (Figs. 1A and 1C) or treated as independent observations (Figs. 1B and 1D). On day 1, median <SUV_{max}>_{pt} was 6.6 g/mL (interquartile range [IQR], 5.6–9.5 g/mL) for the HER2+ group versus 3.7 g/mL (IQR, 3.3–4.1 g/mL) for the HER2- group (*P* < 0.005). On day 2, the corresponding values were 6.8 (IQR, 6.0–9.4) and 4.3 (IQR, 4.1–4.9) g/mL (*P* < 0.005). For individual tumors, the median SUV_{max} for HER2+ and HER2- patients was 7.0 (IQR, 4.8–10.6) and 3.7 (IQR, 3.0–4.7) g/mL, respectively, on day 1 (*P* < 0.001), and 8.7 (IQR, 5.7–13.0) and 4.6 (IQR, 3.8–5.0) g/mL, respectively, on day 2 (*P* < 0.001). Within the HER2+ and HER2- classifications, differences in <SUV_{max}>_{pt} and SUV_{max} distributions between any of the positive IHC/FISH subgroups and any of the negative IHC/FISH subgroups were all significant, and IHC1+ was lower than IHC2+/FISH- (*P* < 0.05, Wilcoxon test).

Tumor uptake and tumor-to-nontumor contrast generally increased between day 1 and 2 for both HER2+ and HER2- patients (Fig. 2). For lesions measured both days, SUV_{max} was higher (*P* < 0.001, *t* test) on day 2 than day 1 for 33 of 38 (87%) tumors in HER2+ patients (average % change, 27 ± 24 [mean ± SD]) and 13 of 14 (93%) tumors in HER2- patients (average % change, 36 ± 26), even as blood SUV decreased by 26% ± 9% and 18% ± 4% respectively, in the 2 groups.

Tumor uptake varied more among and within HER2+ than HER2- patients (Fig. 1). The variance of <SUV_{max}>_{pt} was 30-fold greater for HER2+ than HER2- patients on day 1 (*P* < 0.005) and 56-fold greater on day 2 (*P* < 0.001). For patients with more than 1 measured lesion, inpatient coefficients of variation for SUV_{max} were 40% ± 15% (mean ± SD) and 32% ± 15%, respectively, for HER2+ and HER2- patients on day 1 (*P* = not significant) and 37% ± 16% and 20% ± 2%, respectively, on day 2 (*P* < 0.05).

The <SUV_{max}>_{pt} and SUV_{max} distributions for HER2+ and HER2- patients overlapped substantially (Fig. 1). For days 1 and 2, respectively, 1 and 3 patients classified as HER2+ had lower <SUV_{max}>_{pt} than the highest patient classified as HER2-. On days 1 and 2, respectively, 47% and 43% of the SUV_{max} measurements for the HER2+ group were lower than the highest SUV_{max} for the HER2- group.

Overlap of the uptake distributions for the HER2+ and HER2- groups is exemplified in Figure 3, in which images of a HER2+ patient (IHC3+) and a HER2- patient (IHC1+) are compared. Both had lesions at or near the surface of a breast that were well visualized by PET/CT 1 d after injection of ⁶⁴Cu-DOTA-trastuzumab and for which SUV_{max} was similar.

Tumor Uptake Compared Between ⁶⁴Cu-DOTA-Trastuzumab and ¹⁸F-FDG

There was no significant difference in tumor uptake of ¹⁸F-FDG between HER2+ and HER2- patients (median <SUV_{max}>_{pt}, 8.5 [IQR, 6.6–10.9] and 8.7 [IQR, 5.4–10.7] g/mL, respectively). Neither same-lesion (SUV_{max}) nor same-patient (<SUV_{max}>_{pt}) uptake was correlated between ¹⁸F-FDG and ⁶⁴Cu-DOTA-trastuzumab.

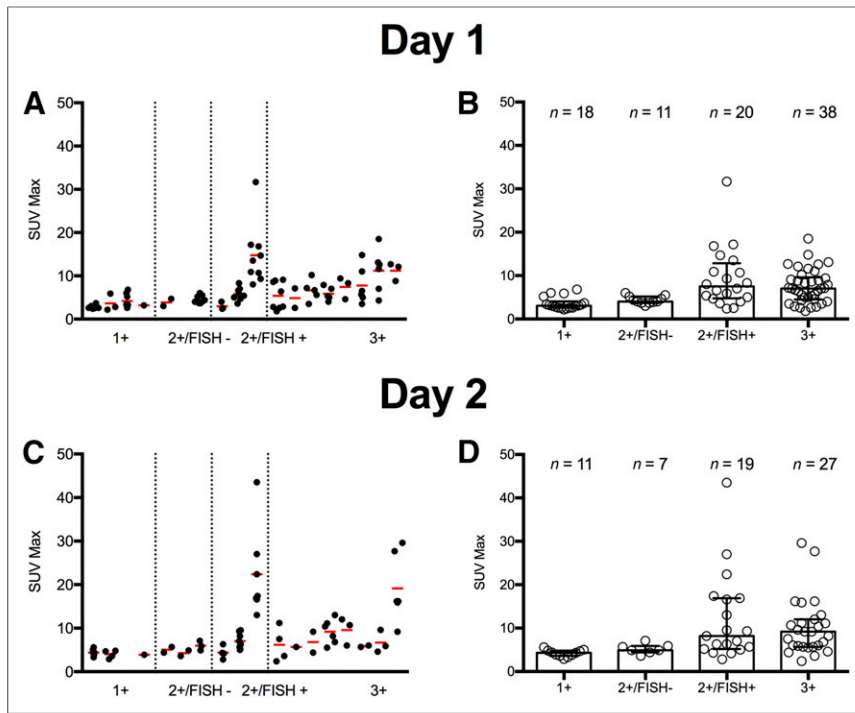


FIGURE 1. Tumor uptake (SUV_{max}) of ^{64}Cu -DOTA-trastuzumab versus patient IHC/FISH score from biopsied tumor. Data are from ^{64}Cu -DOTA-trastuzumab PET/CT scans acquired 1 d (A and B) and 2 d (C and D) after injection. In A and C, the data for individual tumors (black dots) are grouped by patient and IHC/FISH score. Inpatient means are represented by red horizontal lines. In B and D, SUV_{max} for individual lesions (open circles) are combined across patients and grouped by IHC/FISH score (n = number of tumors per group). Intragroup medians are represented as amplitudes of rectangular overlays; error bars denote first and third quartiles. In both analyses, tumor uptake is generally higher for the HER2+ subgroups (3+ or 2+/FISH+) ($P < 0.005$). Relative variability of uptake was greater for HER2+ than HER2- group, both among ($P < 0.001$) and within ($P < 0.05$ on day 2) patients.

DISCUSSION

The half-life of ^{64}Cu (13 h) is short relative to the pharmacokinetics of antibodies. However, for ^{64}Cu -DOTA-trastuzumab in MBC, our observations show that most tumors are well visualized with PET and uptake is indicative of binding to HER2 within 1 d after injection, even in patients classified as HER2-. All patients in the study had at least low-level (IHC1+) expression of HER2 in a biopsied tumor. Measured tumor uptake was positively correlated with patient HER2 status as defined by guidelines of the American Society of Clinical Oncology/College of American Pathologists (1). Furthermore, SUV_{max} increased between day 1 and day 2 for the preponderance of tumors measured on both days.

It is generally agreed that tumor uptake is best measured after most of the radiotracer has left the blood, at which time uptake is near maximal and most accurately reflects binding to the molecular target (9). For antibodies, such late-phase imaging necessitates a radiolabel half-life of several days or more, leading some investigators to prefer ^{89}Zr (half-life, 3.3 d) as the PET radiolabel.

Several clinical investigations with ^{89}Zr -trastuzumab in MBC have been reported. Gebhart et al. (10) grouped 56 HER2+ patients according to the proportion of ^{18}F -FDG-avid tumors showing ^{89}Zr -trastuzumab uptake greater than blood-pool activity. Their findings (29% negative, 25% positive, 46% heterogeneous) are similar to our observations with ^{64}Cu -DOTA-trastuzumab in

HER2+ patients (Fig. 1C; details in the supplemental materials). Ulaner et al. (11) measured SUV_{max} in 9 patients with HER2- primary tumors. Five tumors (each in a different patient) were positively imaged with ^{89}Zr -trastuzumab; SUV_{max} for those are consistent with ours (details in the supplemental materials). Interestingly, only the 2 tumors with lowest SUV_{max} were HER2+ on subsequent histopathology, thus demonstrating that trastuzumab uptake is not equivalent to HER2 expression.

Our work implies that trastuzumab binding in MBC is sufficiently rapid that visualization and measurement of HER2-specific uptake can be achieved for most tumors within 1–2 d after injection. This is significant for PET imaging of trastuzumab with respect to both patient radiation dose and clinical applicability. The radiation dose necessary to obtain good-quality tumor images and uptake measurements may be much lower with the shorter-lived ^{64}Cu radiolabel (7,12). However, this results from being able to image effectively at 1–2 d, rather than from the difference in radioisotope decay rates. If the disease burden is unlikely to be obscured by activity in adjacent blood vessels, ^{89}Zr -trastuzumab PET/CT can also be performed 1–2 d after injection, with concomitant reduction of injected activity. Furthermore, a shorter examination period is a significant advantage in the context of patient treatment schedules.

We observed large variability in tumor uptake of ^{64}Cu -DOTA-trastuzumab both among and within patients. We previously showed that, in MBC, ^{64}Cu -DOTA-trastuzumab $\langle SUV_{max} \rangle_{pt}$ is linearly correlated with average number of HER2 gene copies per tumor cell ($\langle \#HER2 \text{ copies/cell} \rangle_{pt}$) as measured by FISH, and that the wide range of ^{64}Cu -DOTA-trastuzumab uptake among HER2+ patients (5-fold in the current study) likely reflects variation in tumor HER2 expression driven by gene amplification (13). However, HER2 expression does not fully explain the observed heterogeneity, given that some patients have substantially higher $\langle SUV_{max} \rangle_{pt}$ than others with lower $\langle \#HER2 \text{ copies/cell} \rangle_{pt}$. Patients might be misclassified because of biopsy sampling error resulting from heterogeneous intratumoral distribution of HER2. Similarly, inpatient heterogeneity of ^{64}Cu -DOTA-trastuzumab uptake (up to 5-fold in the current study) might result from variable HER2 expression among different tumors. However, the existing evidence indicates a low incidence of intratumoral and inpatient heterogeneity of HER2 expression (14,15). Physiologic barriers against antibody delivery to cells within solid tumors have been well-documented in xenografted models (6), but their clinical importance remains largely unexplored.

One way of investigating the role of physiologic barriers is to examine the lesion site dependence of trastuzumab uptake (Supplemental Fig. 2). Unfortunately, our study is not fully representative of the anatomic sites of MBC. None of the patients had active metastasis to the brain, and only 3 patients (all HER2+) had

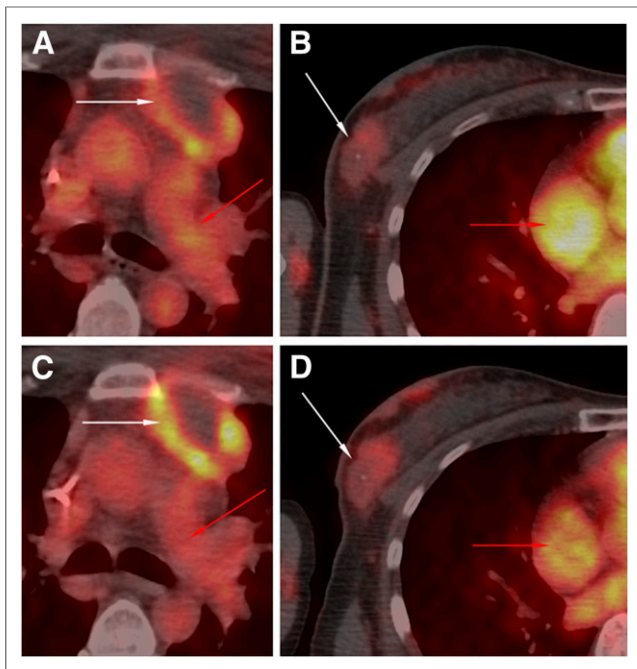


FIGURE 2. Examples of increased tumor uptake and tumor-to-non-tumor contrast between 1 and 2 d after injection of ^{64}Cu -DOTA-trastuzumab. White and red arrows, respectively, denote tumors and blood pool as seen in transaxial PET/CT fusion images. Images on left are from a HER2+ (IHC2+/FISH+) patient. A (day 1) and C (day 2) show large metastasis in prevascular lymph node for which uptake was concentrated at tumor surface. Upper intensity threshold (white color) corresponds to $\text{SUV} = 22 \text{ g/mL}$. At times of the 2 scans (24 and 48 h), measured SUV_{max} for tumor was 17 and 27 g/mL , respectively, whereas SUV for blood was 15 and 11 g/mL . Right-hand column depicts metastatic mass in right breast of a HER2- patient (IHC1+). Upper intensity threshold for images (white color) was set at $\text{SUV} = 10 \text{ g/mL}$. SUV_{max} for tumor increased from 2.6 to 5.0 g/mL between day-1 (25 h after injection) (B) and day-2 (49 h after injection) (D) scans, whereas SUV for blood declined from 12 to 8.8 g/mL .

evaluable liver metastases (6 in total). Although the data suggest higher uptake in the liver lesions, there were no statistically significant differences among lesion sites for either HER2+ or HER2- patients.

Measurement error contributes variability and bias to PET measurements of radiopharmaceutical uptake. In particular, the partial-volume effect causes negative bias with magnitude inversely related to object size (8). In the current study, evaluated lesions were, on average, larger for the HER2- than the HER2+ patients (Supplemental Fig. 1). However, the partial-volume effect would have tended to decrease values measured in HER2+ relative to HER2- patients. Thus, its potential influence does not detract from the conclusion that, on average, tumor uptake of the antibody was higher in the HER2+ than the HER2- group.

Whatever the causes, the observed heterogeneity in tumor uptake of the radiolabeled antibody implies a potential role for ^{64}Cu -DOTA-trastuzumab PET/CT in patient selection and treatment design for therapy that includes trastuzumab. The variability in uptake seen among women with HER2+ MBC is reminiscent of the limited rates of response in such patients (3), whereas the observation that uptake in some HER2- patients exceeded that in some HER2+ patients is consistent with the fact that some

HER2- patients benefit from treatment with trastuzumab (4). The point is that, unlike histopathology, ^{64}Cu -DOTA-trastuzumab PET/CT measures trastuzumab dose to tumor after intravenous administration and, therefore, may improve prediction of response to and benefit from the antibody over histopathology alone. Furthermore, individualized treatment design could be enabled by measurement of trastuzumab uptake at different sites of metastasis within a single patient.

A key question not addressed in the current study is whether tumor uptake of ^{64}Cu -DOTA-trastuzumab is actually correlated with tumor response or patient benefit. Trastuzumab is usually combined with chemotherapy, obscuring the effects of the antibody. For the antibody-drug conjugate T-DM1 on the other hand, uptake of trastuzumab is the primary determinant of therapeutic dose to tumor. Others have shown that tumor uptake of ^{89}Zr -trastuzumab, assessed by qualitative inspection of PET/CT images, is highly accurate in predicting early response to T-DM1 in HER2+ MBC (10). We are currently evaluating ^{64}Cu -DOTA-trastuzumab PET/CT for prediction of response and benefit for women receiving T-DM1 as second-line treatment for HER2+ MBC. A question explored in that study is whether a threshold for tumor uptake of ^{64}Cu -DOTA-trastuzumab can be established below which the likely benefit from T-DM1 therapy is no greater than from alternative treatments.

CONCLUSION

Uptake of ^{64}Cu -DOTA-trastuzumab in MBC was strongly associated with patient HER2 status by 1 d after injection and increased between days 1 and 2 in most tumors for both HER2+ and HER2- patients. These observations imply that ^{64}Cu -DOTA-trastuzumab uptake in MBC is indicative of binding to HER2

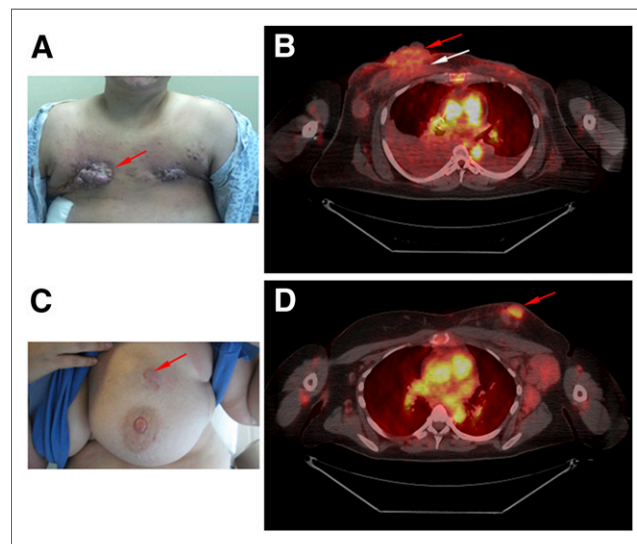


FIGURE 3. Examples of tumor visualization with ^{64}Cu -DOTA-trastuzumab PET/CT. Scan images are transaxial PET/CT fusion images with upper intensity thresholds (white color) corresponding to $\text{SUV} = 10 \text{ g/mL}$. Patient depicted in A and B had recurrent disease after double mastectomy that was scored IHC1+. Scanning began 21 h after injection. Measured SUV_{max} was 6.9 g/mL for lesion in surface of right breast (red arrow) and 6.0 g/mL for mass beneath it (white arrow). Patient shown in C and D had widespread metastatic disease scored as IHC3+. Scanning, begun 25 h after injection, showed SUV_{max} of 7.0 g/mL in tumor at and near surface of left breast (arrows).

within 24 h after injection. Tumor uptake varied widely among and within patients classified as HER2+, and the distributions of inpatient average and individual tumor SUV_{max} overlapped substantially between HER2+ and HER2- patients. This suggests a role for ⁶⁴Cu-DOTA-trastuzumab PET/CT in optimizing treatments that include trastuzumab.

DISCLOSURE

Joanne E. Mortimer is a consultant for Puma Pharmaceuticals. This study was funded by Department of Defense grant BC095002 (Joanne E. Mortimer, principal investigator). The production of ⁶⁴Cu at Washington University School of Medicine is supported by the Department of Energy. Research reported in this publication included work performed in the City of Hope Clinical Pathology and Biostatistics Cores supported by the National Cancer Institute of the National Institutes of Health under award number P30CA033572. The content is solely the responsibility of the authors and does not necessarily represent the official views of the National Institutes of Health. No other potential conflict of interest relevant to this article was reported.

ACKNOWLEDGMENTS

Image analysis utilized customized software provided by Mirada Medical, Oxford, England. We especially thank Mirada Medical U.S. Support Manager Jennifer Miller for her assistance in implementing and maintaining the software.

REFERENCES

1. Wolff AC, Hammond MEH, Hicks DG, et al. Recommendations for human epidermal growth factor receptor 2 testing in breast cancer: American Society of Clinical Oncology/College of American Pathologists clinical practice guideline update. *J Clin Oncol*. 2013;31:3997–4013.
2. Giordano SH, Temin S, Kirshner JJ, et al. Systemic therapy for patients with advanced human epidermal growth factor receptor 2-positive breast cancer: American Society of Clinical Oncology clinical practice guideline. *J Clin Oncol*. 2014;32:2078–2099.
3. Nielsen DL, Kümler I, Palshof AE, Andersson M. Efficacy of HER2-targeted therapy in metastatic breast cancer: monoclonal antibodies and tyrosine kinase inhibitors. *Breast*. 2013;22:1–12.
4. Pogue-Geile KL, Kim C, Jeong J-H, et al. Predicting degree of benefit from adjuvant trastuzumab in NSABP trial B-31. *J Natl Cancer Inst*. 2013;105:1782–1788.
5. Singh JC, Jhaveri K, Esteva FJ. HER2-positive advanced breast cancer: optimizing patient outcomes and opportunities for drug development. *Br J Cancer*. 2014;111:1888–1898.
6. Jain RK. Delivery of molecular and cellular medicine to solid tumors. *Adv Drug Deliv Rev*. 2012;64(suppl):353–365.
7. Mortimer JE, Bading JR, Colcher DM, et al. Functional imaging of human epidermal growth factor receptor 2-positive metastatic breast cancer using ⁶⁴Cu-DOTA-trastuzumab PET. *J Nucl Med*. 2014;55:23–29.
8. Boellaard R, Krak NC, Hoekstra OS, Lammertsma AA. Effects of noise, image resolution, and ROI definition on the accuracy of standard uptake values: a simulation study. *J Nucl Med*. 2004;45:1519–1527.
9. van Dongen GAMS, Visser GM, Lub-de Hooge MN, Vries EG, Perk LR. Immuno-PET: a navigator in monoclonal antibody development and applications. *Oncologist*. 2007;12:1379–1389.
10. Gebhart G, Lamberts LE, Wimana Z, et al. Molecular imaging as a tool to investigate heterogeneity of advanced HER2-positive breast cancer and to predict patient outcome under trastuzumab emtansine (T-DM1): the ZEPHIR trial. *Ann Oncol*. 2016;27:619–624.
11. Ulaner GA, Hyman DM, Ross DS, et al. Detection of HER2-positive metastases in patients with HER2-negative primary breast cancer using ⁸⁹Zr-trastuzumab PET/CT. *J Nucl Med*. 2016;57:1523–1528.
12. Laforest R, Lapi SE, Oyama R, et al. [⁸⁹Zr]trastuzumab: evaluation of radiation dosimetry, safety, and optimal imaging parameters in women with HER2-positive breast cancer. *Mol Imaging Biol*. 2016;18:952–959.
13. Bading J, Press M, Villalobos I, et al. Tumor uptake of ⁶⁴Cu-DOTA-trastuzumab correlates with HER2 gene amplification in patients with metastatic breast cancer [abstract]. *J Nucl Med*. 2016;57(suppl 2):25P.
14. Rossi S, Basso M, Strippoli A, et al. Hormone receptor status and HER2 expression in primary breast cancer with synchronous axillary metastases or recurrent metastatic disease. *Clin Breast Cancer*. 2015;15:307–312.
15. Allott EH, Geradts J, Sun X, et al. Intratumoral heterogeneity as a source of discordance in breast cancer biomarker classification. *Breast Cancer Res*. 2016;18:68.